Shallow water table effects on water, sediment, and pesticide transport in vegetative filter strips - Part 2: model coupling, application, factor importance, and uncertainty

Claire Lauvernet, R Munoz Carpena

Hydrol. Earth Syst. Sci., 22, 71–87, 2018
https://doi.org/10.5194/hess-22-71-2018

Hydrology and Earth System Sciences
Open Access
EGU

Shallow water table effects on water, sediment, and pesticide transport in vegetative filter strips – Part 2: model coupling, application, factor importance, and uncertainty

Claire Lauvernet[1] **and Rafael Muñoz-Carpena**[2]

[1]Irstea, UR MALY, centre de Lyon-Villeurbanne, 5 Rue de la Doua, CS 20244, 69625 Villeurbanne Cedex, France
[2]University of Florida, Agricultural and Biological Engineering, 287 Frazier Rogers Hall,
P.O. Box 110570 Gainesville, FL 32611-0570, USA

Correspondence: Claire Lauvernet (claire.lauvernet@irstea.fr)

Received: 8 July 2017 – Discussion started: 23 August 2017
Revised: 2 November 2017 – Accepted: 9 November 2017 – Published: 5 January 2018

Abstract. Vegetative filter strips are often used for protecting surface waters from pollution transferred by surface runoff in agricultural watersheds. In Europe, they are often prescribed along the stream banks, where a seasonal shallow water table (WT) could decrease the buffer zone efficiency. In spite of this potentially important effect, there are no systematic experimental or theoretical studies on the effect of this soil boundary condition on the VFS efficiency. In the companion paper (Muñoz-Carpena et al., 2018), we developed a physically based numerical algorithm (SWINGO) that allows the representation of soil infiltration with a shallow water table. Here we present the dynamic coupling of SWINGO with VFSMOD, an overland flow and transport mathematical model to study the WT influence on VFS efficiency in terms of reductions of overland flow, sediment, and pesticide transport. This new version of VFSMOD was applied to two contrasted benchmark field studies in France (sandy-loam soil in a Mediterranean semicontinental climate, and silty clay in a temperate oceanic climate), where limited testing of the model with field data on one of the sites showed promising results. The application showed that for the conditions of the studies, VFS efficiency decreases markedly when the water table is 0 to 1.5 m from the surface. In order to evaluate the relative importance of WT among other input factors controlling VFS efficiency, global sensitivity and uncertainty analysis (GSA) was applied on the benchmark studies. The most important factors found for VFS overland flow reduction were saturated hydraulic conductivity and WT depth, added to sediment characteristics and VFS dimensions for sediment and pesticide reductions. The relative importance of WT varied as a function of soil type (most important at the silty-clay soil) and hydraulic loading (rainfall + incoming runoff) at each site. The presence of WT introduced more complex responses dominated by strong interactions in the modeled system response, reducing the typical predominance of saturated hydraulic conductivity on infiltration under deep water table conditions. This study demonstrates that when present, the WT should be considered as a key hydrologic factor in buffer design and evaluation as a water quality mitigation practice.

1 Introduction

Today, surface waters are threatened by pesticide pollution on local, regional, and global scales (Malaj et al., 2014; Stehle and Schulz, 2015). Agricultural surface runoff (RO) is an important contributor to this contamination (Louchart et al., 2001). Grass buffer zones or vegetative filter strips (VFSs), are a typical environmental control practice to protect aquatic ecosystems from sediment, and agrichemicals from agricultural fields (Roberts et al., 2012). While VFSs are recommended in the USA and other regions, in Europe they are often mandatory along rivers due to their potential to limit surface pesticide runoff and aerial spray drift from entering adjacent surface water bodies (Asmussen et al., 1977; Rohde et al 1980; USDA-NRCS, 2000; Dosskey, 2001; Syversen and Bechmann, 2004; Poletika et al., 2009). However, the effectiveness of edge-of-field buffer strips to

reduce runoff transport of pesticides can be very different as a function of many local characteristics (land use, soil, climate, vegetation, and pollutants). For example, based on 16 field studies (Reichenberger et al., 2007), the 25th percentile of VFS pesticide reduction efficiency ranges from 45 to 75 % of the amount coming into the filter from the field edge.

Moreover, VFSs are typically located down the hillslope along the hydrographic network. As a result, the filter is often bounded by a seasonal shallow or perched water table (WT), which may significantly inhibit their function and must be taken into account when designing VFSs and evaluating their efficiency (Lacas et al., 2005). Dosskey et al. (2001, 2006) identified the presence of shallow water table (< 1.8 m) as an important factor that should be considered for VFS design and evaluation. Simpkins et al. (2002) also report that the hydrogeologic setting, specifically the direction of groundwater flow and the position of the water table in thin sand aquifers underlying the buffers, is probably the most important factor in determining buffer efficiency. Arora et al. (2010), in a review on VFS pesticide retention from agricultural runoff, found that soil saturation from a shallow water table may be a reason for negative runoff volume retention. Other studies also identify the potential effects of location of the buffers where a shallow water table is present (Ohliger and Schulz, 2010; Borin et al., 2004) but do not quantify or study its effects (Lacas et al., 2005).

The processes occurring in the VFSs interact in a complex manner in space and time, and thus they must be simulated by dynamic models accounting for hydrologic (Gatel et al., 2016) and sedimentological variability (Fox et al., 2005). The Vegetative Filter Strip Modeling System (VFSMOD) (Muñoz-Carpena et al., 1993, 1999; Muñoz-Carpena and Parsons, 2004) is a storm-based numerical model coupling overland flow, water infiltration, and sediment trapping in a filter considering incoming surface flow and sediment from an upslope field (Fig. 1). VFSMOD also includes a generalized empirical pesticide trapping equation as a function of soil and sediment sorption, dissolved phase infiltration, and sorbed phase sedimentation (Sabbagh et al., 2009). Pesticide degradation on the filter is included between runoff events for long-term pesticide assessments (Muñoz-Carpena et al., 2015), but neglected during events due to their short duration (minutes to hours). VFSMOD has been successfully tested against measured data for predictions of flow, infiltration, and sediment trapping efficiency (Muñoz-Carpena et al., 1999; Abu-Zreig, 2001; Dosskey et al., 2002; Fox et al., 2005; Han et al., 2005; Pan et al., 2017); tracers and multireactive solutes (Perez-Ovilla, 2010); phosphorus (Kuo and Muñoz-Carpena, 2009); pesticides (Poletika et al., 2009; Sabbagh et al., 2009; Winchell et el., 2011); and colloids (Yu et al., 2013). Previous work studied the global sensitivity of simulated outflow, sediment, and pesticide trapping to VFSMOD input factors (Muñoz-Carpena et al., 2007, 2010, 2015; Fox et al., 2010). On the watershed scale, VFSMOD has been included in methods or frameworks to optimize filter placement and design (Dosskey et al., 2006; Tomer et al., 2009; White and Arnold, 2009; Balderacchi et al., 2016; Carluer et al., 2017). Sabbagh et al. (2010) integrated VFSMOD within higher-tier, US EPA long-term pesticide exposure framework (PRZM/VFSMOD/EXAMS) to estimate changes in aquatic concentrations when VFSs are adopted as a runoff pollution control practice. Recently, the German environmental protection agency (UBA) developed the GERDA software package as a pesticide regulatory tool for surface water that includes VFSMOD simulations with a shallow water table where present (Bach et al., 2017).

The extended Green–Ampt soil infiltration component (Skaggs and Khaheel, 1982) used in VFSMOD does not account for the presence of a shallow water table. In a companion paper (Muñoz-Carpena et al., 2018), a physically based algorithm was developed to describe soil infiltration under shallow water table conditions (SWINGO: Shallow Water table INfiltration alGOrithm). Dynamic coupling of this new infiltration algorithm in VFSMOD will allow for mechanistic description of interactions between surface and subsurface hydrology under shallow water table boundary conditions and ensuing effects on VFS sediment and pesticide transport.

Thus, the objective of this work is to study the effects that the change in infiltration introduced by the presence of shallow water table has on VFS runoff reduction, sediment and pesticide trapping. This was done by (a) dynamic coupling of SWINGO in VFSMOD, (b) applying the coupled model on two contrasted and realistic benchmark study sites (sandy-loam soil vs. silty-clay soil) and events (Mediterranean semi-continental vs. temperate oceanic climates), and (c) global sensitivity and uncertainty analysis to ascertain the actual global importance of shallow water table depth on the efficiency of the VFS when compared to other input factors.

2 Material and methods

2.1 Dynamic coupling of shallow water table infiltration algorithm (SWINGO) with VFSMOD overland flow, sediment, and pesticide components

The overland flow submodel in VFSMOD (Muñoz-Carpena et al., 1993a) (Fig. 1) is based on the kinematic wave equation numerical, upwinding Petrov–Galerkin finite element (FE) solution (Lighthill and Whitham, 1955),

$$\begin{cases} \dfrac{\partial h_s}{\partial t} + \dfrac{\partial q}{\partial x} = i - f = i_e \\ S_f \approx S_o \rightarrow q = \dfrac{\sqrt{S_o}}{n} h_s^{\frac{5}{3}} \end{cases}, \quad (1)$$

with initial and boundary conditions

$$\begin{cases} h_s = 0; 0 \le x \le VL, t = 0 \\ h_s = h_{so}; x = 0, t \ge 0 \end{cases}, \quad (2)$$

where $h_s = h_s\,(x, t)$ (L) is the overland flow depth, t is time (T), $q = q\,(x, t)$ ($L^2\,T^{-1}$) is discharge per unit width, x (L)

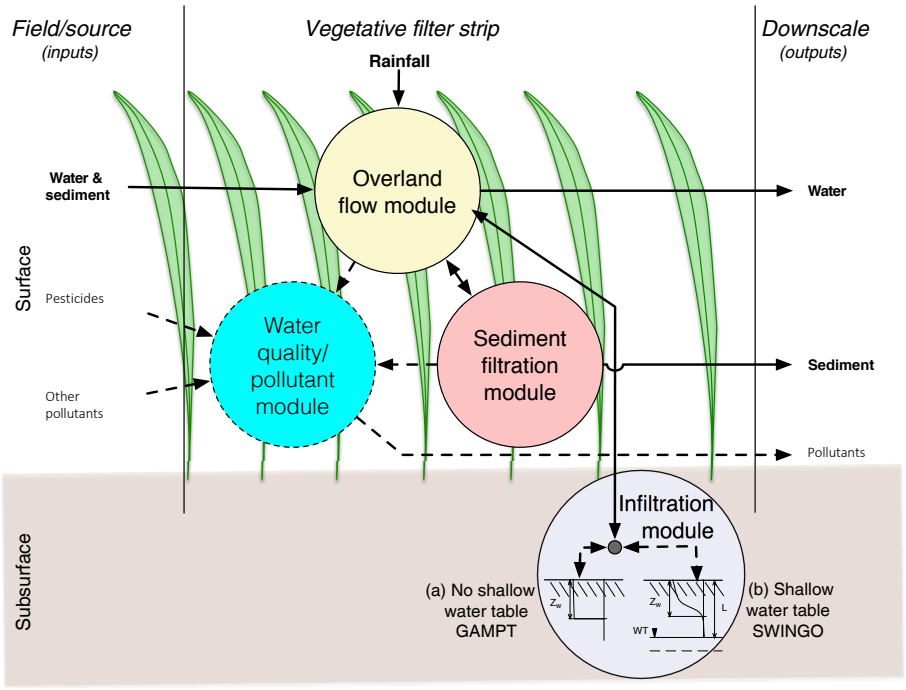

Figure 1. Conceptual model of VFSMOD showing the coupling between overland flow, soil infiltration and redistribution, sediment, and pesticide components. Solid lines indicate required processes and their interactions, and dashed lines are optional, user-selected components. The selection of infiltration under either **(a)** a deep water table (extended Green–Ampt, GAMPT), or **(b)** a shallow water table (SWINGO) is highlighted.

is the surface flow direction axis, $i = i(t)$ (LT^{-1}) is rainfall intensity, $f = f(t)$ (LT^{-1}) is soil infiltration rate, $i_e = i_e(t)$ (LT^{-1}) is rainfall excess, S_o and S_f (LL^{-1}) are the bed and water surface friction slopes at each node of the system, n is Manning's surface roughness coefficient, VL (L) is the filter length, and $h_{so} = h_{so}(0,t)$ (L) represents the field run-on hydrograph entering the filter as a boundary condition (Fig. 2).

Originally, the overland flow component was coupled for each time step with a modified Green–Ampt infiltration algorithm for unsteady rainfall (GAMPT, see Fig. 1) for soils without a (or with a deep) water table (Chu, 1978; Mein and Larson, 1971, 1973; Skaggs and Khaheel, 1982; Muñoz-Carpena et al., 1993b). The infiltration component provides the rainfall excess, i_e in Eq. (1), based on a given unsteady rainfall distribution (hyetograph) for each FE node and time step. The field conditions can be well represented since the program handles field inflow hydrographs and hyetographs, as well as spatial variability of the filter over the nodes of the grid (Fig. 2).

In the sediment component (Fig. 1), based on sediment mechanics (transport and deposition) in shallow flow, the model divides the incoming sediment into bed load (coarse particles, with diameter $>37\,\mu m$) and suspended load (fine particles, diameter $<37\,\mu m$). Bed load deposition is dynamically calculated based on Einstein's bed load transport equation successfully tested for variable shallow flow through nonsubmerged dense vegetation (Barfield et al., 1978). Transport and deposition of suspended particles is calculated for nonsubmerged dense vegetation conditions (Tollner et al., 1976; Wilson et al., 1981). Flow characteristics needed for sediment calculations are provided for each time step by the overland flow component. The particle deposition pattern on the filter is predicted based on a conceptual sediment wedge, mass-balance approach (Fig. 2a).

Pesticide reduction and transport in the filter during the runoff event is calculated within the water quality–pollutant module (Fig. 1) based on a generalized regression-based approach developed from a large database of field studies by Sabbagh et al. (2009) and further tested by others (Poletika et al., 2009; Winchell et al., 2011). The equation considers reduction of dissolved pesticides through infiltration, deposition of sediment-bound pesticides, and pesticide adsorption characteristics. The integration of the mechanistic (flow and sedimentation from VFSMOD) and empirical pesticide approaches allows for identification of important site-specific factors determining the efficiency of pesticide removal (or lack thereof) under realistic field conditions (Muñoz-Carpena et al., 2010; Fox et al., 2010).

In this work, to simulate VFS water, sediment, and pesticide dynamics under realistic unsteady rainfall-runoff conditions for shallow water table conditions, we dynamically couple the new algorithm SWINGO (developed in the com-

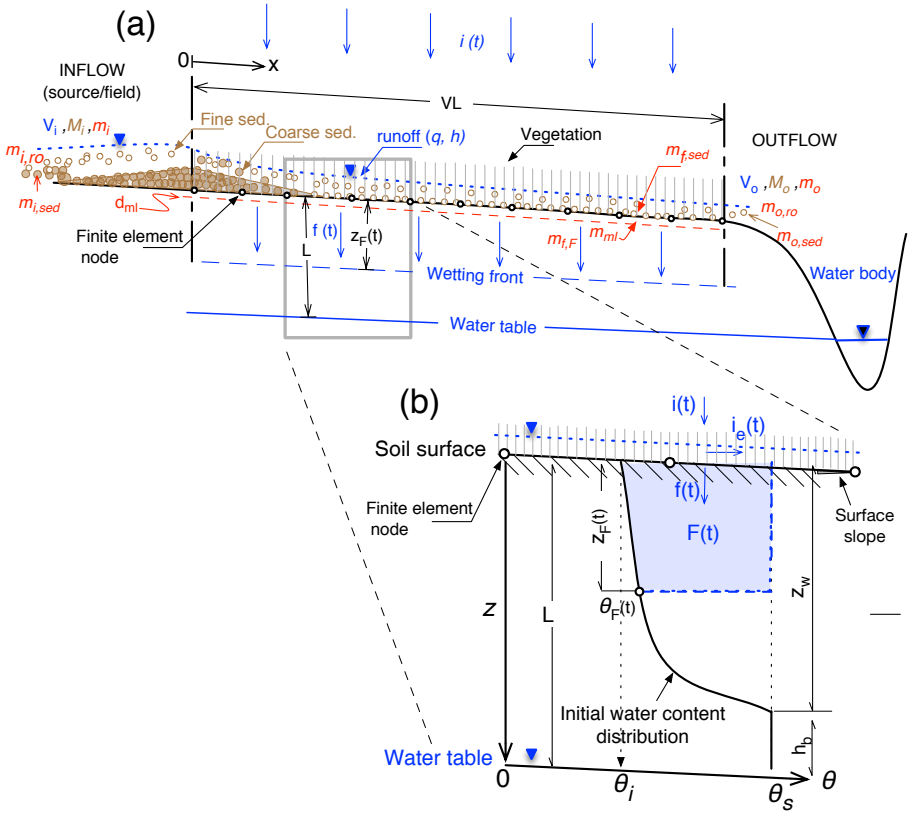

Figure 2. Details of the dynamic coupling of **(a)** the overland flow and sediment and pesticide transport through the VFS (contained in VFSMOD), with **(b)** the new infiltration and soil water redistribution with shallow water component (SWINGO). Colors indicate water (blue), sediment (brown), and pesticide (red) components. V, M, and m indicate water, sediment, and pesticide mass moving through the filter, where subscripts indicate incoming (i), outgoing (o), in sediment (sed), on the filter (f), infiltrated (F), in mixing layer (ml), and in runoff (ro). Other symbols are defined in the text.

panion paper; Muñoz-Carpena et al., 2018) as an alternative, user-selected infiltration submodel (Fig. 1). Full details of SWINGO are provided in the companion paper (Muñoz-Carpena et al., 2018). Briefly, SWINGO is a time-explicit infiltration solution based on a combination of approaches by Salvucci and Entekhabi (1995) and Chu (1997) with the assumption of a horizontal wetting front. Proposed integral formulae allow estimation of the singular times: time of ponding (t_p), shift time (t_0), and time (t_w) when the wetting front depth is equal to z_w (capillary fringe above the water table, Fig. 2b). As with GAMPT, the algorithm provides the infiltration rate f (Eq. 1) for each FE node and time step in VFSMOD as follows:

$$\begin{cases} f = i & 0 < t < t_p \\ f = f_p = K_s + \dfrac{1}{z_F}\displaystyle\int_0^{L-Z_F} K(h)\,dh & t_p < t < t_w \\ f = \min(f_w, i) & t \geq t_w \end{cases}, \quad (3)$$

where (Fig. 2b), z (L) is the vertical axis, z_F (L) is wetting front depth from the surface, L (L) the depth to the water table, $K = K(h)$ (MT^{-1}) the soil water hydraulic conductivity function of soil matric suction h (L) (nonuniform with depth), K_s (MT^{-1}) is the saturated hydraulic conductivity, and f_w (MT^{-1}) is the end soil boundary condition when the wetting front reaches the water table (or its capillary fringe) typically assumed as vertical saturated flow or lateral drainage (see companion paper for details; Muñoz-Carpena et al., 2018). For real VFS field situations, unsteady rainfall without initial ponding must be considered and t_p and t_0 calculated. For each time step increment, $\Delta t = t_j$-t_{j-1}, the surface water balance at each VFS FE node (neglecting evaporation during the event) (Chu, 1997) is

$$\Delta P = \Delta F + \Delta s + \Delta \mathrm{RO}, \quad (4)$$

where ΔP, ΔF, Δs, and ΔRO (L) are changes for each Δt of cumulative precipitation (P), cumulative infiltration (F), surface storage, and cumulative runoff (RO). Notice that $i_e = \Delta \mathrm{RO} / \Delta t$ for each time step. Unsteady rainfall is described by a hyetograph of constant i_j for each rainfall period. If surface storage becomes $s = 0$ then t_p and t_0 are re-calculated at the next rainfall period as follows:

$$t_p = \frac{1}{i}(\theta_s z_p - \int_0^{z_p} \theta(L - z)dz), \quad (5)$$

where θ_s, $\theta(h)$ ($L^3\,L^{-3}$) are the soil water saturated content and the soil water characteristic curve, and z_p (L) is the equivalent wetting front depth at t_p, and for periods after the first, $z_F(t)$ (Fig. 2b) is calculated explicitly from the Newton–Raphson iterative solution (k iteration level):

$$\left.\begin{aligned} G(z_F) &= t - t_p + t_0 - \int_0^{z_F} \frac{\theta_s - \theta(L-z)}{K_s - \frac{1}{z_F}\int_L^{z_F} K(L-z)\mathrm{d}z}\mathrm{d}z \\ G'(z_F) &= -\frac{\theta_s - \theta(L-z)}{K_s - \frac{1}{z_F}\int_L^{z_F} K(L-z)\mathrm{d}z} \end{aligned}\right| \Rightarrow$$

$$z_F^{k+1} = z_F^k - \frac{G(z_F^k)}{G'(z_F^k)} \text{ with } \left|z_F^{k+1} - z_F^k\right| < \varepsilon. \quad (6)$$

with ϵ the convergence tolerance. Finally, the algorithm computes t_w, the time to reach column saturation as follows:

$$t_w = t_p - t_0 + \int_0^{z_w} \frac{1}{f_p}\left[\theta_s - \theta(L-z)\right]\mathrm{d}z. \quad (7)$$

Similarly, this singular time t_w has to be obtained again each time t_p and t_0 are computed. When initial ponding is present we get $t_p = t_0 = 0$. Additional details are provided in the companion paper (Muñoz-Carpena et al., 2018), and Supplement S1 provides instructions for downloading the free VFSMOD open-source code, documentation, and sample applications.

2.2 Benchmark field studies

VFSMOD extended for a shallow water table was applied to two experimental VFS sites in France (Fig. 3, Table 1), selected because they represent contrasting agronomic, pedological, and climatic conditions (Fontaine, 2010). The first site in a Beaujolais vineyard (Rhône-Alpes) consists of a vegetative filter strip on a steep hillslope (20–30 %) located along the river Morcille (affluent of the Saône river). The site was instrumented from 2001 to 2008 for long-term experiments of infiltration–percolation of crop protection products (Boivin et al., 2007; Lacas, 2005; Lacas et al., 2012). The region has a semicontinental climate, with Mediterranean influence, where intense seasonal runoff events can induce erosion. The soil is a very permeable granitic sandy clay. The water table is deep in summer and shallow in winter after intense storm events, from 0.60 m deep at the downstream part of the strip near the river to 4.0 m deep at the field upstream side of the strip (Lacas, 2005).

The site of Jaillière (Loire-Atlantique, close to Brittany) is an experimental farm maintained by ARVALIS–Institut du Végétal where soils are shallow and hydromorphic, and climate is temperate oceanic with mild and rainy winters and cool and wet summers (Madrigal-Monarrez, 2004). Buffer zone experiments were conducted at the site under natural rainfall (Patty et al., 1997) and simulated runoff (Souiller et al., 2002). Crops are mainly wheat and maize, typically under tile drainage conditions, with slopes of around 3 %. Silty

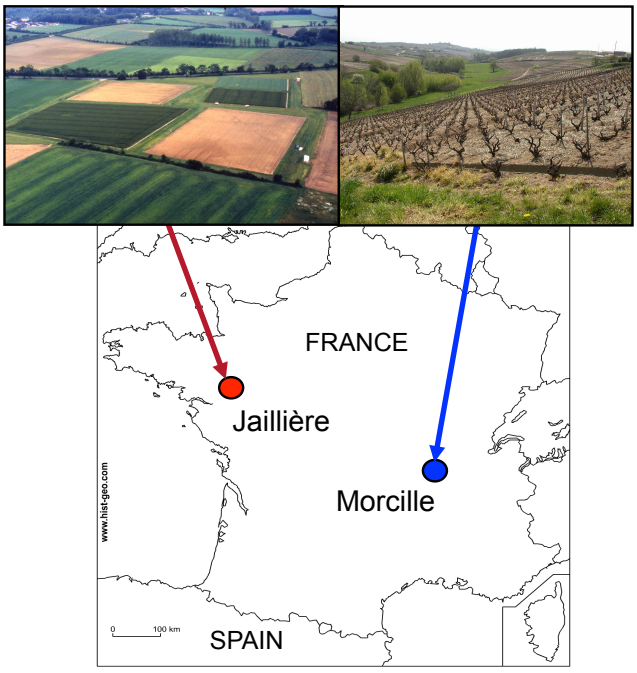

Figure 3. Location of experimental VFS sites: Jaillière, northwestern France, maize crops on a flat silty-clay soil in a temperate oceanic climate; Morcille, southeastern France, vineyards on a sandy-loam soil in a Mediterranean semicontinental climate. Jaillière is located at 47°27′6.25″ N, 0°57′58.37″ W and Morcille is located at 46°10′31.3″ N, 4°38′11.2″ E, in GPS coordinates.

clay soils overlay a virtually impermeable layer of alterite shales, typically leading in winter to the formation of a seasonal shallow water table from 0.5 to 2 m and the appearance of runoff by subsaturation (Adamiade, 2004). This site is also the basis for the EU pesticide regulatory scenario for surface water FOCUSsw D5 (EU-FOCUS, 2001).

Among the pesticides used at the experimental sites, a soluble and low sorption (mobile) herbicide (isoproturon) used on both sites was selected for simulations, contrasted by a less mobile product chosen at each site, i.e., the fungicide tebuconazole at Morcille and the herbicide diflufenican at Jaillière (Madrigal et al., 2002) (Table 1).

While both Morcille and Jaillière provide sufficient details for application of the coupled model (field parameters, initial and boundary conditions), VFS outflow was only available for Morcille. In particular, Lacas (2005) and Lacas et al. (2012) monitored the effectiveness of the VFS at Morcille, but because of the high permeability of the soil and deeper shallow water conditions, only 5 out of the 24 natural rainfall events recorded generated outflow from the VFS. From these 5, the one closer to the average for the high water table season was selected for application of the model (Fig. 4a). Earlier studies at Jaillière by Patty et al. (1997) monitored VFS efficiency in the same site but in the absence of a shallow water table. Although they provide some of the model inputs they

Table 1. Characteristics of the field studies utilized for sensitivity–uncertainty analyses of shallow water table effects on VFS performance.

Study	Authors	Lacas (2005), Lacas et al. (2012)	Madrigal-Monarrez (2004), Adamiade (2004)
	Location, climate	Morcille, Mediterranean semicontinental	Jaillère, temperate oceanic
Event description	Rainfall (mm)	15	10.7
	Rainfall duration (h)	2.1	3
	Inflow volume (mm)	0.847	6.347
	Inflow duration (h)	2.1	7.9
	Hydraulic loading (rainfall + incoming runoff) (m^3)	2.48	25.9
	Shallow water table depth (m)	2.5 (0.4–2.5)	0.8 (0.4–2)
	Source field area (m^2)	2500	4000
Soil description	USDA soil taxonomy	Cambisol luvic	Stagnic luvisol
	USDA texture	Sandy loam	Silty clay
VFS description	Length (direction of flow) × width	6 × 4 m	5 × 10 m
	Slope	28 %	4 %
	Field-to-filter area ratio	1 : 110	1 : 100
	Vegetation	Ray grass (20 years)	Ray grass (7 years)
Pesticides (K_{oc}, mL g^{-1})		Isoproturon (144) Tebuconazole (769)	Isoproturon (144) Diflufenican (3000)

are not directly applicable for this WT model application. Later, working on the same watershed, Branger et al. (2009) and Fontaine (2010) studied the shallow water table effects on runoff at the edge of the field and a receiving drainage ditch, but did not monitor the efficiency of the VFSs. We selected one average event (dynamics and volume) in the middle of the high-water season based on Fontaine (2010) for our model application (Fig. 4b).

To our knowledge there are no VFS experimental studies with a shallow water table present that can be used for systematic model testing. While this paper focuses on coupling of the new infiltration algorithm with VFSMOD and the analysis of the important factors controlling VFS efficiency in the presence of WT, we used the single event with sufficient hydrological data at Morcille to get a preliminary assessment of whether the model responds in the same range as the measured field data. Uncalibrated or "cold" testing of the model (without initial calibration using field values) was performed and the 95 % confidence interval (gray area in Fig. 4a) was obtained by varying only K_s within measured field values (Table 2). The model performance was assessed against the measured data based on FitEval software (Ritter and Muñoz-Carpena, 2013). FitEval uses block-bootstrapping of the observed and predicted paired values to approximate the underlying distributions of goodness-of-fit statistics (Nash–Sutcliffe efficiency, NSE, and root mean square error, RMSE). From these distributions, median values and 95 % confidence intervals (95CI) are provided for both NSE and RMSE. NSE provides a dimensionless metric of goodness of fit, and RMSE an indicator of absolute error, with the same dimensions as model outputs. The uncertainty in the observed data is accounted for in FitEval using the modification of the NSE based on the probable error range (PER) method (Harmel et al., 2007).

2.3 Global sensitivity analysis

Global sensitivity analysis (GSA) and uncertainty analysis (UA) of the coupled model allows for the systematic study of the influence of the input factors and their interactions on VFS performance for surface runoff, sediment, and pesticide removal. The "global" term denotes that GSA studies output variability when all input factors vary globally, within their validity domain defined by probability distribution functions (PDFs), as opposed to locally, (one at a time), i.e., around an arbitrary range from a base value. GSA allows for simultaneous estimation of the factors individual importance and interactions (Saltelli et al., 2004). In this study, two complementary sensitivity methods were used: the qualitative Morris (1991) elementary effects screening method, and the quantitative variance-decomposition extended Fourier amplitude sensitivity test (eFAST) (Cukier et al., 1978; Saltelli et al., 1999). In both methods, input factors are sampled, the model is evaluated on the sample sets, and global sensitivity indices are computed. Morris is generally used as a first, qualitative step to identify a group of important input factors,

Table 2. Input-factor base values and selected statistical distributions at the case study sites.

Input factor (units)	Description	Morcille		Jaillière	
		Base value	Distribution[2]	Base value	Distribution[2]
Hydrological inputs					
FWIDTH (m)	Effective flow width of the strip	4.0	U (4.0, 4.4)	10.0	U (9.0, 10.0)
VL (m)	Length in the direction of the flow	6.0	U (5.4, 6.0)	5.0	U (5.0, 5.5)
RNA ($s\,m^{-1/3}$)	Filter Manning's roughness n for each segment	0.2	T (0.1, 0.2, 0.3)	0.2	T (0.1, 0.2, 0.3)
SOA (–)	Filter slope for each segment	0.25	U (0.20, 0.30)	0.03	U (0.02, 0.04)
VKS ($m\,s^{-1}$)	Soil vertical saturated hydraulic conductivity in the VFS	4.58×10^{-5}	LN (−10.6676, 0.69)	2.50×10^{-6}	LN (13.0, 0.69)
SAV (m)	Green–Ampt's average suction at wetting front	0.110	U (0.088, 0.132)	0.1668	U (0.13, 0.20)
OI (–)	Initial soil water content, θ_i	0.22	U (0.1, 0.35)	0.15	U (0.12, 0.18)
OS (–)	Saturated soil water content, θ_s	0.4	N (0.4, 0.03)	0.4	N (0.4, 0.03)
SCHK (–)	Relative distance from the upper filter edge where check for ponding conditions is made (i.e., 1 = end; 0 = beginning)	0.5	U (0, 1)	0.5	U (0, 1)
L (m)[1]	Shallow water table depth from soil surface	1.0	U (0.4, 2.5)	0.8	U (0.4, 2)
OR (–)[1]	Residual soil water content, θ_i	0.038	N (0.038, 0.03)	0.07	N (0.07, 0.03)
VGALPHA (m^{-1})[1]	van Genuchten soil characteristic curve parameter (α)	10.0	N (10,2)	1.18	N (1.18,0.05)
VGN (–)[1]	van Genuchten soil characteristic curve parameter (n), $m = 1 - 1/n$	1.52	N (1.52, 0.05)	1.45	N (1.45, 0.05)
Vegetation inputs					
SS (cm)	Average spacing of grass stems	1.6	U (1.3, 2.1)	1.6	U (1.3, 2.1)
VN ($s\,cm^{-1/3}$)	Filter media (grass) modified Manning's nm (cylindrical = 0.012)	0.012	T (0.0084, 0.012, 0.016)	0.012	T (0.0084, 0.012, 0.016)
H (cm)	Filter grass height	15.0	U (10, 35)	15.0	U (10, 35)
Sedimentation inputs					
VN2 ($s\,m^{-1/3}$)	Bare surface Manning's n for sediment inundated area in VFS	0.013	T (0.011, 0.013, 0.04)	0.02	T (0.011, 0.02, 0.04)
DP (cm)	Sediment particle size diameter (d50)	0.0099	U (3.80×10^{-3}, 1.60×10^{-2})	0.0029	U ($2.00E \times 10^{-4}$, 3.69×10^{-3})
COARSE (–)	Fraction of incoming sediment with particle diameter > 0.0037 cm (coarse fraction routed through wedge as bed load) (unit fraction, i.e., 100 % = 1.0)	0.55	U (0.51, 0.6)	0.45	U (0.4, 0.49)
Pesticide inputs					
KOC ($ml\,g^{-1}$)	Organic carbon sorption coefficient for simulated pesticide				
Isoproturon		144	T (36, 144, 241)	144	T (36, 144, 241)
Tebuconazole		769	T (102, 769, 1249)	–	–
Diflufenican		–	–	3000	T (1622, 3000, 7431)
PCTOC (%)	Percentage of organic carbon in the soil	1.2	U (1.18, 2.5)	3.78	U (1.4, 7)
PCTC (%)	Percentage clay in the soil	12	U (11, 15)	22	U (19.8, 25.5)

[1] Parameters of the new infiltration under shallow water table component (SWINGO). [2] Statistics of the assigned distributions, uniform: U (mix, max), triangular: T (min, mean, max), log-normal: LN (μ_y, σ_y), normal: N (μ_x, σ_x). LN and N distributions are truncated between (0.001, 0.999).

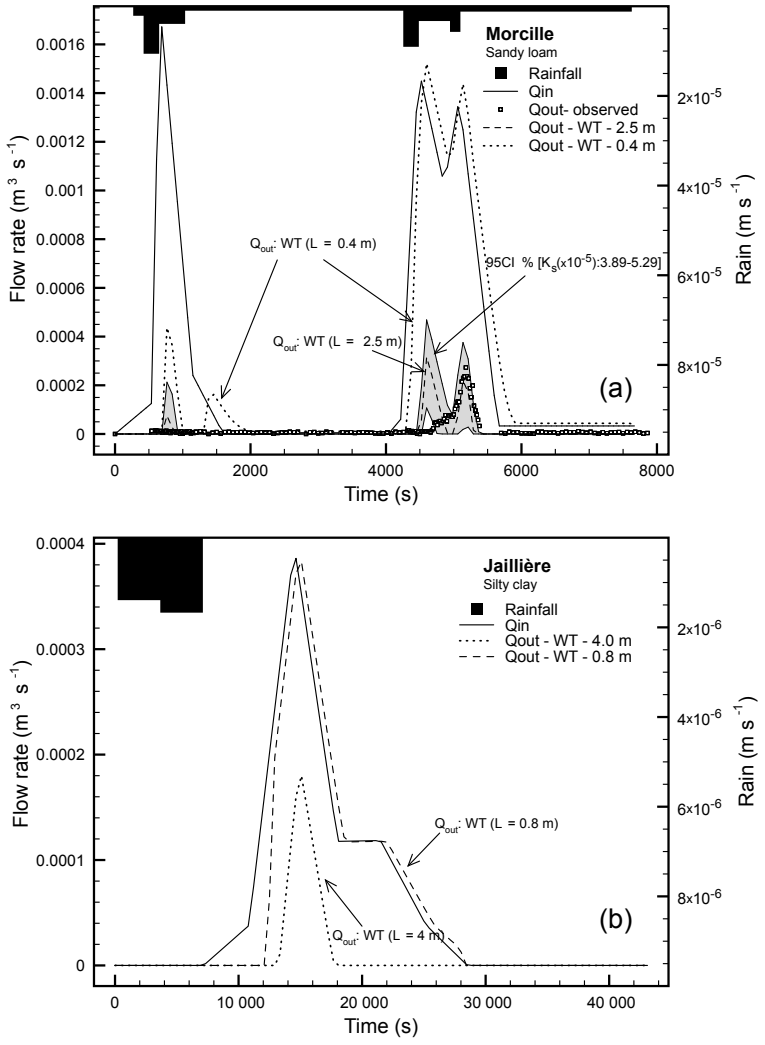

Figure 4. Hydrological response of the VFS at the study sites. **(a)** Event at Morcille 17 August 2004 with $L = 2.5$ m, showing comparison of measured outflow (symbols) and VFSMOD simulations (lines). The dashed Q_{out} line for $L = 2.5$ m corresponds to average conditions for that event ($K_{\text{s}} = 4.58 \times 10^{-5}$ m s^{-1}), and the gray envelope represents outflow variability due to uncertainty of measured hydraulic conductivity. **(b)** Event at Jaillière on 16 February 1997 with $L = 0.8$ m, without outflow measurements. Q_{in} and Q_{out} represent surface inflow and outflow at the VFS. The potential effect on overland outflow of alternative water table depths in those events is represented by the dotted lines for $L = 0.4$ **(a)** and 4.0 m **(b)**.

where in a second step a variance-based method is applied on the selected input factors (Saltelli et al., 2007, 2008).

The Morris method uses in its original form a regular discretization of the k input-factor space defined by their PDFs, requiring a total number of simulations (N) on the order of $N = r(k+1)$, where $r > 8$ is the number of sampling trajectories, typically taken as 10, used here (Campolongo et al., 2007). Each factor influence, called elementary effects (EEs), is evaluated by comparison of simulations where this factor is changed alternatively among the others. Morris is a robust, low-cost sensitivity analysis that allows quick identification of the most influential input factors without prior model assumptions (i.e., linearity, additivity) (Campolongo et al., 2007; Faivre et al., 2013; Khare et al., 2015). Sensitivity indices for each factor X_i ($i = 1, k$) are computed based on the EEs: (i) μ_i^* (mean of absolute values of EEs) that measures *direct effects* of each factor on the output of interest and (ii) σ_i (standard deviation of EEs) that provides a measure of *interactions and nonlinearities*. The method compares the input factors' indices relatively to the others, making possible to visually classify the inputs on a (μ^*, σ) Cartesian plane in four groups as a function of their relative effect on the model: (1) negligible effect (low μ^* and low σ), (2) important direct effects and small interactions (high μ^* and low σ), (3) important nonlinear and/or interactions (high μ^* and high σ),

and (4) interacting factors with low sensitivity (low μ^* and high σ).

The eFAST method is a quantitative global sensitivity method based on high-dimensional variance decomposition. A pseudo-random multivariate sampling scheme is conducted across the k-dimensional space, informed by the input-factor PDFs, requiring $N = M \times k$ simulations with M between 512 and 1024 (8 or 9 binary factor combinations) (Saltelli et al., 2004). The model total output Y variance is decomposed in parts attributed to each factor's direct effects or to factor interactions. First-order sensitivity indices (S_i) for each factor X_i are defined by the fraction of the output variance associated with the direct effect of that factor and represents the average output variance reduction that can be achieved when the input factor X_i is fixed (Tarantola et al., 2002; Yang, 2011). Total sensitivity indices (S_{Ti}) are calculated as the fraction of variance associated with that factor and its interactions. The largest values of the sensitivity indices correspond to the highest influence of these inputs on the corresponding output variable (Saltelli et al., 2008; Faivre et al., 2013). The eFAST method was chosen on this study because it is robust and overcomes the initial limitation of the Fourier amplitude sensitivity test (Cukier et al., 1978), applicable only for mostly additive models (i.e., $\Sigma S_i > 0.6$) (Faivre et al., 2013). The dense variance-based multivariate sampling and ensuing model simulations allow for quantification of the model uncertainty analysis through output probability density functions and statistics (median, quantiles, confidence intervals) (Saltelli et al., 2004; Muñoz-Carpena et al., 2007).

Morris indices (μ^*, σ) have been found to provide a good approximation of the eFAST indices (S_{Ti}, $S_{Ti}-S_i$) at a much lower computational cost (Saltelli et al., 2004; Campolongo et al., 2007), making it ideal for large and computationally expensive models. However, for models with strong nonlinear outputs or discontinuities in the output space, the low density of Morris sampling can result in inaccurate sensitivity analysis results. In this study, both methods were run with the full set of inputs as a check for the consistency and robustness of the GSA results. For conciseness, Morris results are presented in detail and eFAST results are summarized briefly, with additional details in the Supplement.

2.4 Selection of inputs and outputs for GSA simulations

The first step of GSA is to define output variables and input factors. In this study, changes in VFS efficiency were selected as output variables: reduction of water ($\mathrm{d}Q$), sediments ($\mathrm{d}E$), and pesticides ($\mathrm{d}P$). Both model versions, with a water table (SWINGO algorithm) and without a water table (GAMPT algorithm), were compared on each site. The input factors (Table 2) were selected considering previous GSA performed on VFSMOD (Fox et al., 2010; Muñoz-Carpena et al., 2007, 2010), with new inputs for the water table case (OR, VGALPHA and VGN, L, see Tabel 2). Input-factor distributions are assigned based either on experimental measurements on the case study plots, scientific publications, or expert knowledge (Table 2).

Although the VFS dimensions FWIDTH and VL were measured in the field (Table 1), the effective dimensions are known to be different in practice as the runoff does not follow perfectly uniform sheet flow (Abu-Zreig, 2001). Thus, the measured values were chosen to vary uniformly within -10 and $+10$ % for FWIDTH and VL, respectively (Muñoz-Carpena et al., 2010). The slope (SOA) uniform distribution represents field-measured spatial variation across the VFS. PDFs for filter roughness and vegetation factors were assigned based on vegetation type (Table 1) (Haan et al., 1994; Muñoz-Carpena et al., 2007).

For the infiltration components, log-normal PDFs were assigned to the soil saturated hydraulic conductivity (VKS) from measured values at each site (Madrigal-Monarrez, 2004; Souiller et al., 2002; Lacas, 2005) based on effective field values calculated from the harmonic mean of the topsoil horizons (Bouwer, 1969). The Green–Ampt infiltration OI and OS inputs were fitted distributions based on values measured at the sites, and the average suction at the wetting front (SAV) was considered to vary uniformly based on ranges for soil texture at each site (Rawls et al., 1983). Soil water characteristics parameters (VGALPHA, VGN, OR in Table 2) needed for calculation of infiltration under shallow water table (Eqs. 3–7) were assigned normal PDFs based on the soil texture (Meyer et al., 1997). Hourly water table depths (L) that were automatically monitored on the Morcille river during the case study event (Lacas, 2005) followed a uniform distribution. On Jaillière, the average water depth and variation was measured manually at the site (Adamiade, 2004) and a uniform distribution around these values assigned.

Sediment particle characteristics from the upper field (COARSE and DP) were assigned uniform distributions based on USDA textural class (Woolhiser et al., 1990), and truncated to respect the relationship between DP and COARSE (Muñoz-Carpena et al., 1999).

For pesticide inputs, field measurements of the percentage of clay (PTC) and organic carbon (PCTOC) of the upper field followed a uniform PDF (Lacas, 2005; Benoit et al., 1998; Madrigal-Monarrez, 2004). The triangular distribution for KOC for the pesticides evaluated at each site is based on measurements in Jaillière for the base value and boundaries (Benoit et al., 1998; Souiller et al., 2002) and on Morcille for the base value (Lacas, 2005) but using boundaries from the PPDB database (IUPAC, 2007).

In all, for the two sites, two infiltration options (GAMPT, without shallow water table and with $k = 18$, and SWINGO, with shallow water table and with $k = 20$, Table 2) and two pesticides at each site, the total number of GSA simulations performed were 75 544 for eFAST ($M = 497 \approx 512$) and 1600 for Morris. The procedure was repeated 3 times with different random seeds to ensure the robustness of the results.

3 Results

3.1 Model application on benchmark studies

The effect of a water table on simulated VFS efficiency using SWINGO was first tested on the two contrasted benchmark study sites Morcille (Fig. 4a) and Jaillière (Fig. 4b). Since a stream at the bottom of the VFS was present on both sites, the lateral Dupuit–Forscheimer option was selected for the end vertical bottom boundary condition f_w (Eq. 3) (see Sect. 2.1 in companion paper; Muñoz-Carpena et al., 2018), hereon referred to as the vertical boundary condition. The detailed outflow hydrograph from the VFS measured during the event at Morcille is compared with a direct simulation with base values (no calibration) (Fig. 4a). The dashed line for $L = 2.5$ m corresponds to the simulation with average measured VKS for the top soil horizons (4.58×10^{-5} m s^{-1}), and the gray envelope represents outflow variability due to uncertainty of measured hydraulic conductivity (between 3.89×10^{-5} m s^{-1} from direct measurement on the soil surface horizon 10–30 cm and 5.29×10^{-5} m s^{-1} computed by harmonic mean of measurements on 0–10 and 10–30 cm horizons). In addition to the measured water table depth at the sites, each event was tested with different water table conditions to study the expected response to these conditions (Fig. 4a, b). The large differences in VFS surface outflow found between shallow and deeper water tables clearly illustrates the hydrological importance of a shallow water table presence on VFS at these sites.

Direct simulation of the VFS surface outflow at Morcille fits observations well for the end of the second rain period (4000 to 6000 s) but misses the rest (Fig. 4a). The differences between simulated and observed values could come from measurement or parametrization errors at the site, since runoff was expected early on for an event with such hydraulic loading (rainfall + incoming runoff). The intrinsic spatial variability of K_s also represents a significant source of uncertainty in the simulations (gray area in Fig. 4a). The NSE AND RMSE ranges for the model uncertainty bounds in Fig. 4a were median NSE = 0.610 and 95CI [0.448–0.943], and RMSE = 4.284×10^{-5} [1.179×10^{-5}–7.472×10^{-5}] m^3 s^{-1}. Within those uncertainty bounds, the model is classified as "unacceptable" to "very good" based on the FitEval methodology (Ritter and Muñoz-Carpena, 2013). FitEval evaluation files are included in the Supplement. In all, considering that the model was run with base values and without calibration, these preliminary results are deemed promising.

The effect of water table change (from 0–2 m) on VFS changes in runoff (dQ), sediment (dE), and pesticide (dP) reductions for the two case studies is presented in Fig. 5. In general, dQ and dP are sensitive to the shallow water table depth until a threshold (~ 1.5 m for the case study sites) beyond which there are no effects and the filter achieves maximum efficiency for the event. The two-step curves for Morcille are due to the two storm periods, where relative contributions to surface flow between the first and second events will vary with the depth of the shallow water table. Sediment retention (dE) does not exhibit similar changes because the relatively low flow conditions experienced likely result in low available transport capacity and high sediment deposition on the VFS. The difference in effects introduced by the chemical characteristics of the pesticide is observed in the curves for diflufenican (high sorption) and isoproturon (low sorption) at Jaillière. This local study does not take into account all effects and interactions between input factors, but only the water table depth variation effect. The global sensitivity analysis presented in Sect. 3.2 will address this.

The simulation results for Morcille and Jaillière confirm that a shallow water table can affect the VFS surface hydrological response by generating saturation surface runoff, depending on the soil characteristics and the hydraulic loading. Conversely, for deep water table, surface hydrology processes are effectively decoupled after a threshold controlled by the soil characteristics and hydraulic loading. Interestingly, simulations with the option without a shallow water table (GAMPT, Fig. 1) for the case study conditions closely matched those for SWINGO for the deeper water tables in Fig. 4, providing additional physical consistency to both components.

3.2 Global sensitivity analysis of water, sediment, and pesticide reductions

A combination of simulations with a shallow water table ("WT", run with SWINGO) and with no shallow water table ("no WT", run with GAMPT) (Fig. 1) for Jaillière and Morcille conditions, with two pesticides at each site (Table 1), were selected for GSA Morris and eFAST methods. For simplicity, GSA results are presented only for one pesticide, isoproturon, which is a common herbicide with average sorption properties. A comparison of the different pesticides' effects is presented in the Sect. 3.3.

Morris sensitivity analysis indices (Table S1 in the Supplement) are presented in Fig. 6, where important input factors for each output are separated from the origin of the (μ^*, σ) Cartesian planes. Distinct patterns on the important factors controlling the shallow water table effects on the efficiency of the VFS (dQ, dE, dP) are identified by comparing the different soil (fine at Jaillière and coarse at Morcille) and hydraulic loading across the study sites. The differences can be interpreted in terms of the interplay between excess rainfall (controlled mainly by the saturated hydraulic conductivity VKS and hydraulic loading) and subsaturation (i.e., subsurface saturation controlled by the water table depth L).

Finer soils typically exhibit lower permeability but a higher capillarity fringe above a water table (Terzaghi, 1943; Lane and Washburn, 1946; Parlange et al., 1990). For no WT, excess rainfall (controlled by VKS) leads to relatively more water on the surface compared to coarse soils. Morris

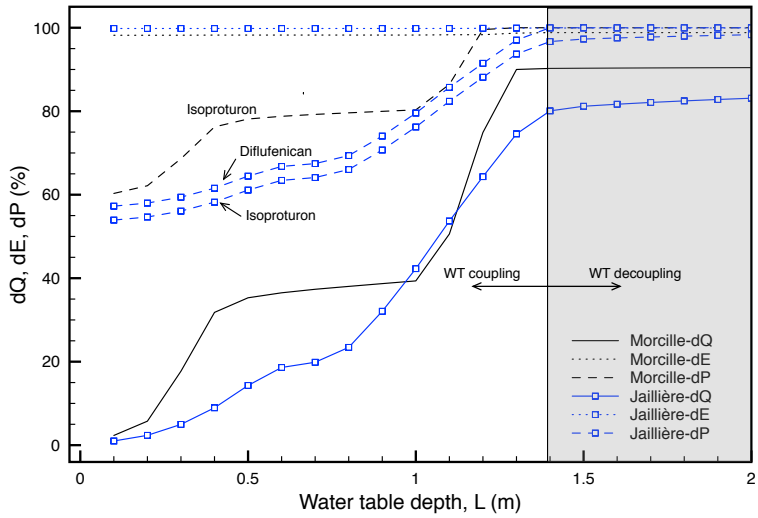

Figure 5. Change in dQ (reduction of surface water), dE (reduction of sediment), and dP (reduction of pesticide isoproturon) with water table depth for experimental events in Fig. 4a–b. Gray area indicates water table depths where influence over surface outputs on the VFS is no longer observed.

results (Fig. 6a) show the strong sensitivity of dQ to VKS for this case. With WT the soil readily saturates from the bottom and it is less sensitive to VKS. This is shown by the strong direct effect of L on dQ (Fig. 6d). For dE in finer soils, more runoff present at the surface typically results in higher available transport capacity, and sediment and surface characteristics become a limiting factor for transport and deposition (Muñoz-Carpena et al., 2010). This is shown by the importance of DP and interaction with VKS (Fig. 6b). With WT, the infiltration is limited even further in these fine soils, where excess rainfall no longer controls surface flow and VKS falls in importance while sediment and surface characteristics dominate the response (Fig. 6e). In general, pesticide reduction (dP) is controlled by factors controlling the liquid (dQ) and solid (dE) phase transport (Sabbagh, et al., 2009). For no WT and for this moderately adsorbed chemical, the effect of excess rainfall on dQ (controlled by VKS) also becomes the most important process for dP (Fig. 6c). With WT, the dominance of L in dQ is also present in dP, with some sediment and pesticide characteristics also showing importance (Fig. 6f).

In contrast, the coarser soil in Morcille exhibits higher permeability and small capillary fringe and, under no-WT runoff, is typically controlled by excess rainfall (importance of VKS in Fig. 6g). With WT, the soil might subsaturate depending on position L, and this input gains importance interacting with VKSs (Fig. 6j). For dE and no WT (Fig. 6h), with more permeability the surface water flow (controlled by VKS) is the main limiting factor controlling sedimentation (Muñoz-Carpena et al., 2010). With WT, again the VKS and L that control surface flow also interact strongly to control sedimentation, and sediment soil water characteristics are of secondary importance (Fig. 6k). Control of infiltration also propagates into dP, and for this moderately sorbed pesticide, dQ factors also control dP (Fig. 6i, l).

Interestingly, introduction of WT increases the number of factors and interactions (i.e., more input factors show higher σ values and are separated near or above the dashed 1 : 1 line). This indicates an increase in complexity of the VFS response when the shallow water table is present. This suggests that simple relationships to simulate water, sediment, and pesticide behavior are not able to represent all complex processes that interact in a VFS.

Comparison of Morris and eFAST indices (Fig. 6, and Table S2 and Fig. S1) for interactions and first-order effects, $S_{Ti} - S_i \sim \sigma$ and $S_{Ti} \sim \mu^*$, respectively, shows good consistency among the methods (Saltelli et al., 2004; Campolongo et al., 2007) and further corroborates the results. The importance of VKS for both soils under no WT identified by Morris is quantified by eFAST with more than 90 % of the dQ and dP output variance being controlled by first-order (direct) effects of this factor (Fig. S1a, g and c, i). Similarly, the importance of DP for dE for the fine soil is apparent where more than 60 % of the variance is explained by first-order and interaction effects of this factor (Fig. S1b, e). For the case of WT, the effect of L on dQ and dP is predominant, with 60–90 % of the output controlled by this factor and its interactions (Fig. S1d, j, l).

3.3 Uncertainty analysis

The model runs from eFAST dense multivariate input sampling allows the realization of a quantitative uncertainty analysis of the model outputs' water (dQ), sediment (dE), and pesticide (dP) reductions for the two contrasted pesticides at each site (Fig. 7 and Table S3). As expected, the reduction

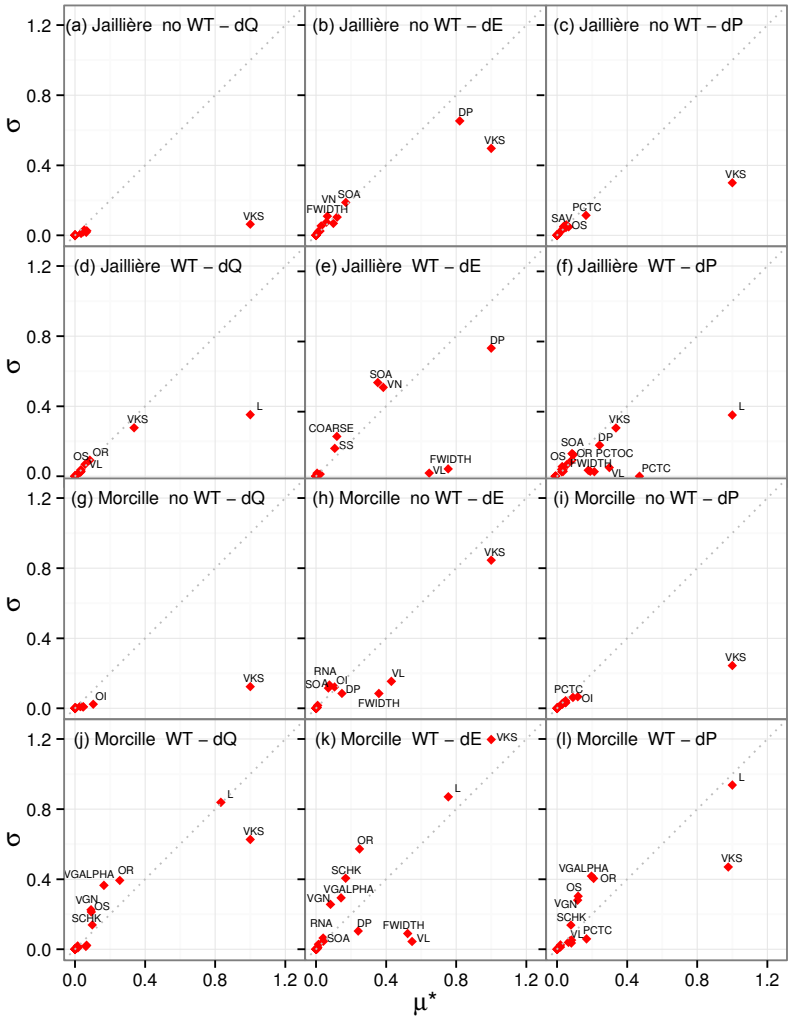

Figure 6. Morris elementary effects results for dQ (reduction of surface water), dE (reduction of sediment), and dP (reduction of pesticide isoproturon) on Jaillière **(a–f)** and Morcille **(g–l)** sites, without water table (no WT) and with water table (WT) present. Factors with negligible effects (close to the origin) are not labeled.

in infiltration and increase in surface flow introduced by the shallow water table translates into a distinct decrease in dQ values, with median dQ changing from 81 to 7 % and 65 to 45 % in Jaillière (Fig. 7a, b) and Morcille (Fig. 7c, d), respectively (Table S3). For dE, for the coarser soil at Morcille the smaller change in dQ with WT does not visibly change the high sediment retention, whereas for the finer soil of Jaillière the changes in flow introduce marked changes in median dE from 99 to 64 %. Again, changes in dQ and dE with WT affect the VFS pesticide retention at both sites, with median reductions from d$P = 99$ to 38 % and 97 to 84 % in Jaillière and Morcille, respectively. Since the VFS pesticide retention is also directly related to pesticide sorption characteristics (Sabbagh et al., 2009), some differences are expected for different chemicals. Reduction of diflufenican at Jaillière (dP-Dif) (Fig. 7b) and tebuconazole at Morcille (dP-Teb) (Fig. 7d) is higher than reductions of the other two pesticides because of their affinity for sediment (higher KOC values in Table 1) and high sediment retention in the VFS.

These results further support the GSA findings that changes in surface and subsurface hydrological responses, introduced by the shallow water table, can translate into important reductions on the expected pesticide retention and uncertainty controlled by field conditions (soils, hydraulic loading, pesticide characteristics).

4 Summary and conclusions

In this study, we coupled a new infiltration algorithm under shallow water table conditions (SWINGO, developed in companion paper; Muñoz-Carpena et al., 2018) with a commonly used event-based vegetative filter strips model (VF-

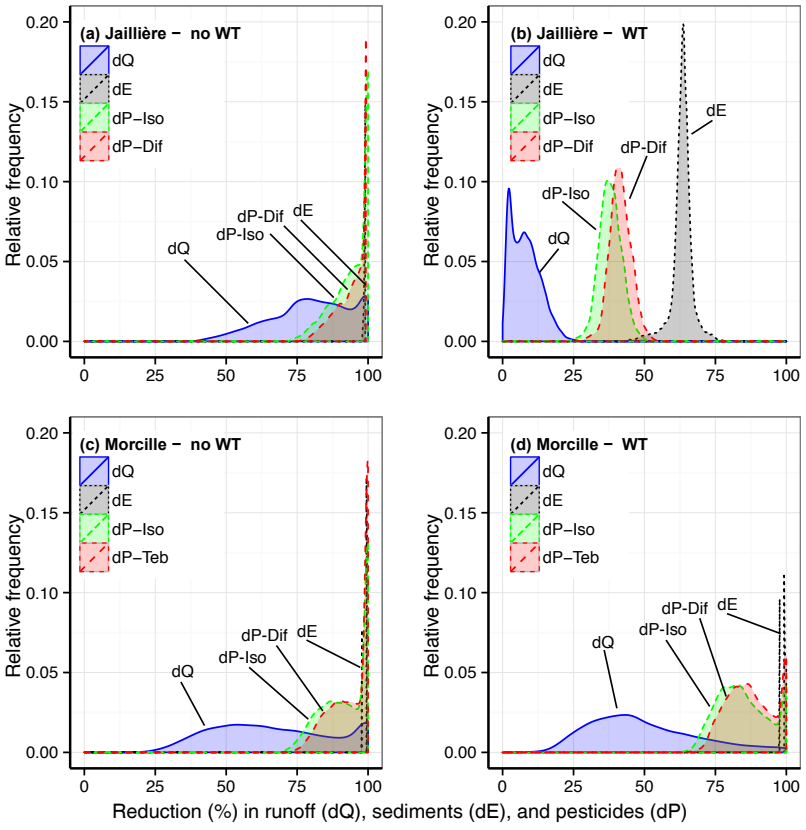

Figure 7. Probability density functions from the uncertainty analysis of eFAST simulations on output variables dQ (reduction of surface water), dE (reduction of sediment), and dP (reduction of pesticides) for the Jaillière **(a–b)** and Morcille **(c–d)** sites, without water table (no WT) and with water table (WT). Pesticides are isoproturon (Iso), diflufenican (Dif), and tebuconazole (Teb).

SMOD). The coupled model takes into account the dynamic interactions among water table, surface runoff, sediment, and pesticide filtration in a vegetative filter strip. The model was applied to two different experimental sites with contrasted soils and rainfall conditions. The direct testing of the uncalibrated model under limited experimental conditions showed promising results. Simulations varying the water table depth for two experimental sites provided interesting insights on the effect on VFS efficiencies to reduce overland flow, sediment, and pesticides. While the VFS surface flow, sediment, and pesticide reduction responses are very sensitive when the water table is close to the surface, the effect is lost after a threshold depth around 1.5 m for the experimental sites condition, consistent with previous field studies (Dosskey et al., 2006; Lacas et al., 2012). For depths larger than the threshold, the model showed physical consistency when compared to a common Green–Ampt solution (with no water table assumptions). More comprehensive global sensitivity and uncertainty analyses for the two sites revealed that the effectiveness of the VFSs was markedly reduced in the presence of the shallow water table, and in this case the VFS response is more complex, dominated by interactions between surface, subsurface, and transport processes. The most important factors controlling the expected variability of water and pesticide reductions are water table depth and saturated hydraulic conductivity of the soil, but their importance also depends on sediment characteristics controlled by the soil type and hydraulic loading of the event. Uncertainty in the pesticide reduction, driven by water or sediment reduction, also depends on the pesticide sorption properties (KOC).

This work suffers from several limitations. Firstly, limited field experimental data is available for detailed studies of the response of a VFS under alternative conditions of deep and shallow water tables. Further laboratory and field research should address this limitation, where exhaustive experimental datasets must be compiled to reduce the uncertainty in the identification of sensitive input factors controlling the measured and simulated responses studied here. To address this limitation, a comprehensive laboratory testing of the updated model under mesoscale controlled shallow water conditions was just presented by Fox et al. (2017), with successful results. Still, field studies under controlled and uncontrolled conditions are recommended to identify strategies for model parametrization and optimal design of VFS under realistic

WT field conditions. Secondly, although two contrasting case studies were selected, the results presented here are limited to these studies, and further analysis will be needed for other local, regional, and larger scales.

The application of the improved VFSMOD under contrasting sets of conditions and physical consistency with other models indicate the robustness of the model for use in VFS sizing and evaluation of potential losses of efficiency under shallow water table conditions. Since VFSs are commonly placed near streams and these areas can suffer seasonal shallow water conditions, this tool fills an important gap in environmental management and analysis. For example, in Europe VFSs are often prescribed along river drainage networks without objective assessment of their efficiency during winter wet periods (Carluer et al., 2017; Bach et al., 2017). In the US, the historical topography-based approach, which links priority for buffers to locations where runoff water converges from uplands and saturates the soil, often results in placement on bottomlands next to streams (Dosskey and Qiu, 2011). Alternative targeted placement of buffers based on soil characteristics and conductivity can improve the efficiency of the buffers (Dosskey et al., 2006). However, both placement methods disregard seasonal shallow water table effects that can now be mechanistically assessed with the improved physical model developed herein. For the case of the regulatory assessment of pesticides, currently long-term exposure frameworks in Europe and the USA disregard the potential effects that shallow water effects might have in reducing the effectiveness of in-label mitigation practices like VFSs. Results from this study support the critical need to incorporate the effects of a shallow water table, when present, in these environmental exposure assessments.

Data availability. Model, code, data and additional materials are publicly accessible through the supplement provided in this paper.

The Supplement related to this article is available online at https://doi.org/10.5194/hess-22-71-2018-supplement.

Author contributions. CL and RMC participated in the model coupling, coding the GSA application, analysis, and interpretation of the results and writing of the paper.

Competing interests. The authors declare that they have no conflict of interest.

Acknowledgements. The authors wish to thank Nadia Carluer for the field testing dataset and selection of the study sites, as well as her review of the paper. Marilisa Letey helped with the literature review for this paper. Axel Ritter helped in the FitEval evaluation of the experimental data. Claire Lauvernet acknowledges TOPPS-PROWADIS for partial project funding. The second author received support from the UF Research Foundation Professorship, UF Water Institute Fellowship, and USDA NIFA Award no. 2016-67019-26855. The authors also thank the University of Florida Research Computing (https://www.rc.ufl.edu) for providing high-performance computational resources and support that have contributed to the research results reported in this publication.

Edited by: Nunzio Romano
Reviewed by: Stefan Reichenberger, Marnik Vanclooster, and one anonymous referee

References

Abu-Zreig, M.: Factors Affecting Sediment Trapping in Vegetated Filter Strips: Simulation Study Using VFSMOD, Hydrol. Process., 15, 1477–1488, https://doi.org/10.1002/hyp.220, 2001.

Adamiade, V.: Influence d'un fossé sur les écoulements rapides au sein d'un versant, Université Pierre et Marie Curie, Spécialité Géosciences – Ressources Naturelles, Paris VI, 238 pp., 2004.

Arora, K., Mickelson, S. K., Helmers, M. J., and Baker, J. L.: Review of Pesticide Retention Processes Occurring in Buffer Strips Receiving Agricultural Runoff1, J. Am. Water Resour. Ass., 46, 618–647, https://doi.org/10.1111/j.1752-1688.2010.00438.x, 2010.

Asmussen, L. E., White, A. W., Hauser, E. W., and Sheridan, J. M.: Reduction of 2,4-D Load in Surface Runoff Down a Grassed Waterway, J. Environ. Qual., 6, 159–162, https://doi.org/10.2134/jeq1977.00472425000600020011x, 1977.

Bach, M., Guerniche, D., Thomas, K., Trapp, M., Kubiak, R., Hommen, U., Klein, M., Reichenberger, S., Pires, J., and Preuß, T.: Bewertung des Eintrags von Pflanzenschutzmitteln in Oberflächengewässer – Runoff, Erosion und Drainage, GERDA – GEobased Runoff, erosion and Drainage risk Assessment for Germany, Umweltbundesamt, Dessau-Roßlau, Germany, ISSN 1862–4359, 2017.

Balderacchi, M., Perego, A., Lazzari, G., Muñoz-Carpena, R., Acutis, M., Laini, A., Giussani, A., Sanna, M., Kane, D., and Trevisan, M.: Avoiding social traps in the ecosystem stewardship: The Italian Fontanile lowland spring, Sci. Total Env., 539, 526–535, https://doi.org/10.1016/j.scitotenv.2015.09.029, 2016.

Barfield, B. J., Tollner, E. W., and Hayes, J. C.: The use of grass filters for sediment control in strip mining drainage, Theoretical studies on artificial media, Pub. no. 35-RRR2-78, Lexington, Ky, University of Kentucky, Institute for Mining and Minerals Research, Vol. I, 1978.

Benoit, P., Barriuso, E., Vidon, P., and Réal, B.: Isoproturon Sorption and Degradation in a Soil from Grassed Buffer Strip, J. Environ. Qual., 28, 121–129, https://doi.org/10.2134/jeq1999.00472425002800010014x, 1998.

Boivin, A., Lacas, J. G., Carluer, N., Margoum, C., Gril, J.-J., and Gouy, V.: Pesticide leaching potential through the soil of a buffer strip in the river Morcille catchment (Beaujolais), XIII Sym-

posium Pesticide Chemistry – Environmental Fate and Human Health, Piacenza, Italie, 2007.

Bouwer, H.: Infiltration of water into nonuniform soil, J. Irr. Drain. Div., 95, 451–462, 1969.

Branger, F., Tournebize, J., Carluer, N., Kao, C., Braud, I., and Vauclin, M.: A simplified modelling approach for pesticide transport in a tile-drained field: The PESTDRAIN model, Agr. Water Manage., 96, 415–428, https://doi.org/10.1016/j.agwat.2008.09.005, 2009.

Carluer, N., Lauvernet, C., Noll, D., and Muñoz-Carpena, R.: Defining context-specific scenarios to design vegetated buffer zones that limit pesticide transfer via surface runoff, Sci. Total Environ., 575, 701–712, https://doi.org/10.1016/j.scitotenv.2016.09.105, 2017.

Chu, S. T.: Infiltration during unsteady rain, Water Resour. Res., 14, 461–466, https://doi.org/10.1029/WR014i003p00461, 1978.

Cukier, R. I., Levine, H. B., and Shuler, K. E.: Nonlinear sensitivity analysis of multiparameter model systems, J. Comput. Phys., 26, 2365–2366, 1978.

Dosskey, M. G.: Toward quantifying water pollution abatement in response to installing buffers on crop land, Environ. Manage., 28, 577–598, https://doi.org/10.1007/s002670010245, 2001.

Dosskey, M. G., Helmers, M. J., Eisenhauer, D. E., Franti, T. G., and Hoagland, K. D.: Assessment of concentrated flow through riparian buffers, J. Soil Water Conserv., 57, 336–343, 2002.

Dosskey, M. G., Helmers, M. J., and Eisenhauer, D. E.: An Approach for Using Soil Surveys to Guide the Placement of Water Quality Buffers, J. Soil Water Conserv., 61, 344–354, 2006.

Dukes, M. D., Evans, R. O., Gilliam, J. W., and Kunickis, S. H.: Effect of Riparian Buffer Width and Vegetation Type on Shallow Groundwater Quality in the Middle Coastal Plain of North Carolina, T. ASABE, 45, 327–336, 2002.

EU-FOCUS: FOCUS Surface Water Scenarios in the EU Evaluation Process under 91/414/EEC, Report of the FOCUS Working Group on Surface Water Scenarios, EC Document Reference SANCO/4802/2001, Version 1.0, January 2011, 245 pp., 2001.

EU-JRC: SIMLAB Version 2.2.1, Simulation Environment for Uncertainty and Sensitivity Analysis, Joint Research Centre of the European Commission, Ispra, Italy, https://ec.europa.eu/jrc/en/samo/simlab (last access: July 2017), 2004.

Faivre, R., Iooss, B., Mahévas, S., Makowski, D., and Monod, H.: Sensitivity Analysis and Exploration of Models, Editions Quae, in French, 2013.

Fontaine, A.: Optimizing the size of grassed buffer strips to limit pesticides transfer from land to surface water in overland flow, Cranfield University, UK, MSc Thesis, 2010.

Fox, A. L., Eisenhauer, D. E., and Dosskey, M. G.: Modeling water and sediment trapping by vegetated filters using VFSMOD: comparing methods for estimating infiltration parameters, ASAE Paper, 2005.

Fox, G., Muñoz-Carpena, R., and Sabbagh, G.: Influence of flow concentration on parameter importance and prediction uncertainty of pesticide trapping by vegetative filter strips, J. Hydrol., 384, 164–173, https://doi.org/10.1016/j.jhydrol.2010.01.020, 2010.

Fox, G., Muñoz-Carpena, R., and Purvis, R.: Controlled laboratory experiments and modeling of vegetative filter strips with shallow water tables, J. Hydrol., 556, 1–9, https://doi.org/10.1016/j.jhydrol.2017.10.069, 2017.

Gatel, L., Lauvernet, C., Carluer, N., and Paniconi, C.: Effect of surface and subsurface heterogeneity on the hydrological response of a grassed buffer zone, J. Hydrol., 542, 637–647, https://doi.org/10.1016/j.jhydrol.2016.09.038, 2016.

Haan, C. T., Barfield, B. J., and Hayes, J. C.: Design hydrology and sedimentology for small catchments, San Diego, California, Academic Press, 1994.

Han, J., Wu, S., and Allan, C.: Suspended sediment removal by vegetative filter strip treating highway runoff, J. Environ. Sci. Health, 40, 1637–1649, https://doi.org/10.1081/ESE-200060683, 2005.

Harmel, R. D. and Smith, P. K.: Consideration of measurement uncertainty in the evaluation of goodness-of-fit in hydrologic and water quality modeling, J. Hydrol., 337, 326–336, 2007

IUPAC: The PPDB Pesticide Properties Database. International Union of Pure and Applied Chemistry (IUPAC), AERU, University of Hertfordshire, UK, http://sitem.herts.ac.uk/aeru/ppdb/en/index.htm (last access: 18 December 2017), 2007.

Johnson, S. R., Burchell, M. R., Evans, R. O., Osmond, D. L., and Gilliam, J. W.: Riparian Buffer Located in an Upland Landscape Position Does Not Enhance Nitrate-Nitrogen Removal, Ecol. Engin., 52, 252–261, https://doi.org/10.1016/j.ecoleng.2012.11.006, 2013.

Khare, Y. P., Muñoz-Carpena, R., Rooney, R. W., and Martinez, C. J.: A multi-criteria trajectory-based parameter sampling strategy for the screening method of elementary effects, Environ. Modell. Softw., 64, 230–239, https://doi.org/10.1016/j.envsoft.2014.11.013, 2015.

Kuo, Y. M. and Muñoz-Carpena, R.: Simplified modeling of phosphorus removal by vegetative filter strips to control runoff pollution from phosphate mining areas, J. Hydrol., 378, 343–354, https://doi.org/10.1016/j.jhydrol.2009.09.039, 2009.

Lacas, J.-G: Processus de dissipation des produits phytosanitaires dans les zones tampons enherbées, Etude expérimentale et modélisation en vue de limiter la contamination des eaux de surface, Unversité Montpellier II, Sciences et techniques du Languedoc, 2005.

Lacas, J.-G., Voltz, M., Gouy, V., Carluer, N., and Gril, J.-J.: Using grassed strips to limit pesticide transfer to surface water: a review, Agron. Sustain. Dev., 25, 253–266, https://doi.org/10.1051/agro:2005001, 2005.

Lacas, J.-G., Carluer, N., and Voltz, M.: Efficiency of a Grass Buffer Strip for Limiting Diuron Losses from an Uphill Vineyard Towards Surface and Subsurface Waters, Pedosphere, 22, 580–592, https://doi.org/10.1016/S1002-0160(12)60043-5, 2012.

Lane, K. S. and Washburn, S. E.: Capillary tests by capillarimeter and by soil filled tubes, Proceedings Highway Research Board, 26, 460–473, 1946.

Lighthill, M. J. and Whitham, C. B.: On kinematic waves: flood movement in long rivers, Proc. R. Soc. Lon. Ser. A, 22, 281–316, 1955.

Louchart, X., Voltz, M., Andrieux, P., and Moussa, R.: Herbicide Transport to Surface Waters at Field and Watershed Scales in a Mediterranean Vineyard Area, J. Environ. Qual., 30, 982–991, 2001.

Madrigal-Monarrez, I.: Sorption of pesticides in soil from grassed and forested buffer zones: the role of organic matter, INAPG PhD Thesis (AgroParisTech), 2004.

Malaj, E., von der Ohe, P. C., Grote, M., Kühne, R., Mondy, C. P., Usseglio-Polatera, P., Brack, W., and Schäfer, R. B.: Organic

chemicals jeopardize the health of freshwater ecosystems on the continental scale, P. Natl. Acad. Sci. USA, 111, 9549–9554, https://doi.org/10.1073/pnas.1321082111, 2014.

Mein, R. G. and Larson, C. L.: Modelling the infiltration component of the rainfall-runoff process, Bulletin 43, University of Minnesota, MN, Water Resources Research Center, 1971.

Meyer, P. D., Rockhold, M. L., and Gee, G. W.: Uncertainty analyses of infiltration and subsurface flow and transport for SDMP sites, report, 1 September, Washington DC, University of North Texas Libraries, Digital Library, available at: www.digital.library.unt.edu/ark:/67531/metadc690558/ (last access: 7 July 2017), 1997.

Muñoz-Carpena, R., Miller, C. T., and Parsons, J. E.: A Quadratic Petrov-Galerkin Solution for Kinematic Wave Overland Flow, Water Resour. Res., 29, 2615–2627, 1993a.

Muñoz-Carpena, R., Parsons, J. E., and Gilliam, J. W.: Numerical Approach to the Overland Flow Process in Vegetative Filter Strips, T. ASABE, 36, 761–770, 1993b.

Muñoz-Carpena, R., Parsons, J. E., and Gilliam, J. W.: Modeling hydrology and sediment transport in vegetative filter strips, J. Hydrol., 214, 111–129, https://doi.org/10.1016/S0022-1694(98)00272-8, 1999.

Muñoz-Carpena, R. and Parsons, J. E.: A design procedure for vegetative filter strips using VFSMOD-W, T. ASAE, 47, 1933–1941, https://doi.org/10.13031/2013.17806, 2004.

Muñoz-Carpena, R., Zajac, Z., and Kuo, Y.-M.: Global sensitivity and uncertainty analyses of the water quality model VFSMOD, T. ASABE, 50, 1719–1732, 2007.

Muñoz-Carpena, R., Fox, G., and Sabbagh, G.: Parameter Importance and Uncertainty in Predicting Runoff Pesticide Reduction with Filter Strips, J. Environ. Qual., 39, 630–641, https://doi.org/10.2134/jeq2009.0300, 2010.

Muñoz-Carpena, R., Ritter, A., Fox, G. A., and Perez-Ovilla, O.: Does mechanistic modeling of filter strip pesticide mass balance and degradation affect environmental exposure assessments?, Chemosphere, 139, 410–421, https://doi.org/10.1016/j.chemosphere.2015.07.010, 2015.

Muñoz-Carpena, R., Lauvernet, C., and Carluer, N.: Shallow water table effects on water, sediment, and pesticide transport in vegetative filter strips – Part 1: nonuniform infiltration and soil water redistribution, Hydrol. Earth Syst. Sci., 22, 53–70, https://doi.org/10.5194/hess-22-53-2018, 2018.

Ohliger, R. and Schulz, R.: Water body and riparian buffer strip characteristics in a vineyard area to support aquatic pesticide exposure assessment, Sci. Total Environ., 408, 5405–5413, https://doi.org/10.1016/j.scitotenv.2010.08.025.

Pan, D., Gao, X., Dyck, M., Song, Y., Wu, P., and Zhao, X.: Dynamics of runoff and sediment trapping performance of vegetative filter strips: Run-on experiments and modeling, Sci. Total Environ., 593/594, 54–64, https://doi.org/10.1016/j.scitotenv.2017.03.158, 2017.

Parlange, J.-Y., Haverkamp, R., Starr, J. L., Fuentes, C., Malik, R. S., Kumar, S., and Malik, R. K.: Maximal capillary rise flux as a function of height from the water table, Soil Sci., 150, 896–898, 1990.

Patty, L., Réal, B., and Gril, J. J.: The use of grassed buffer strips to remove pesticides, nitrate and soluble phosphorus compounds from runoff water, Pestic. Sci., 243, 243–251, 1997.

Perez-Ovilla, O.: Modeling runoff pollutant dynamics through vegetative filter strips: a flexible numerical approach, Ph.D. Thesis, University of Florida, Gainesville, 195 pp., 2010.

Poletika, N. N., Coody, P. N., Fox, G. A., Sabbagh, G. J., Dolder, S. C., and White, J.: Chlorpyrifos and Atrazine Removal from Runoff by Vegetated Filter Strips: Experiments and Predictive Modeling, J. Environ. Qual., 38, 1042–1052, https://doi.org/10.2134/jeq2008.0404, 2009.

Rawls, W. J., Brakensiek, D. L., and Miller, N.: Green-Ampt infiltration parameters from soils data, J. Hydraul. Eng., 109, 62–70, 1983.

Reichenberger, S., Bach, M., Skitschak, A., and Frede, H.-G.: Mitigation strategies to reduce pesticide inputs into ground- and surface water and their effectiveness: a review, Sci. Total Environ., 384, 1–35, https://doi.org/10.1016/j.scitotenv.2007.04.046, 2007.

Ritter, A. and Muñoz-Carpena, R.: Predictive ability of hydrological models: objective assessment of goodness-of-fit with statistical significance, J. Hydrol., 480, 33–45, https://doi.org/10.1016/j.jhydrol.2012.12.004, 2013.

Roberts, W. M., Stutter, M. I., and Haygarth, P. M.: Phosphorus Retention and Remobilization in Vegetated Buffer Strips: A Review, J. Environ. Qual., 41, 389–399, https://doi.org/10.2134/jeq2010.0543, 2012.

Rohde, W. A., Asmussen, L. E., Hauser, E. W., and Wauchope, R. D.: Trifluralin movement in runoff from a small agricultural watershed, J. Environ. Qual., 9, 37–42, 1980.

Sabbagh, G. J., Fox, G. A., Kamanzi, A., Roepke, B., and Tang, J.-Z.: Effectiveness of Vegetative Filter Strips in Reducing Pesticide Loading: Quantifying Pesticide Trapping Efficiency, J. Environ. Qual., 38, 762–771, https://doi.org/10.2134/jeq2008.0266, 2009.

Saltelli, A., Tarantola, S., and Chan, K. P.-S.: A Quantitative Model-Independent Method for Global Sensitivity Analysis of Model Output, Technometrics, 41, 39–56, 1999.

Saltelli, A., Tarantola, S., Campolongo, F., and Ratto, M.: Sensitivity Analysis in Practice: A Guide to Assessing Scientific Models, John Wiley & Sons, Chichester, 2004.

Saltelli, A., Ratto, M., Andres, T., Campolongo, F., Cariboni, J., Gatelli, D., Saisana, M., and Tarantola, S.: Global Sensitivity Analysis: The Primer, John Wiley & Sons, Chichester, 2008.

Saltelli, A., Annoni, P., Azzini, I., Campolongo, F., Ratto M., and Tarantola, S.: Variance Based Sensitivity Analysis of Model Output, Design and Estimator for the Total Sensitivity Index, Comput. Phys. Commun., 181, 259–270, 2010.

Simpkins, W., Wineland, T., Andress, R., Johnston, D., Caron, G., Isenhart, T., and Schultz, R.: Hydrogeological constraints on riparian buffers for reduction of diffuse pollution: examples from the Bear Creek watershed in Iowa, USA, Water Sci. Technol., 45, 61–68, 2002.

Skaggs, R. W. and Khaheel, R.: Infiltration, chap. 4, in: Hydrologic modeling of small watersheds, edited by: Haan, C. T., Johnson, H. P., and Brakensiek, D. L., St. Joseph, MI, ASAE, 121–168, 1982.

Souiller, C., Coquet, Y., Pot, V., Benoit, P., Réal, B., Margoum, C., Laillet, B., Labat, C., Vachier, P., and Dutertre, A.: Capacités de stockage et d'épuration des sols de dispositifs enherbés vis-à-vis des produits phytosanitaires, Première partie: Dissipation des produits phytosanitaires à travers un dispositif enherbé; mise en évidence des processus mis en jeu par simulation de ruisselle-

ment et infiltrométrie, Etude et Gestion des Sols, 9, 269–285, 2002.

Stehle, S. and Schulz, R.: Agricultural insecticides threaten surface waters at the global scale, P. Natl. Acad. Sci. USA, 112, 5750–5755, https://doi.org/10.1073/pnas.1500232112, 2015.

Syversen, N. and Bechmann, M.: Vegetative buffer zones as pesticide filters for simulated surface runoff, Ecol. Engin., 22, 175–184, 2004.

Tarantola, S., Giglioli, N., Jesinghaus, J., and Saltelli, A.: Can Global Sensitivity Analysis Steer the Implementation of Models for Environmental Assessments and Decision-Making?, Stoch. Env. Res. Risk A., 16, 63–76, 2002.

Terzaghi, K.: Theoretical soil mechanics, Wiley, New York, 1943.

Tollner, E. W., Barfield, B. J., Haan, C. T., and Kao, T. Y.: Suspended sediment filtration capacity of simulated vegetation, T. ASAE, 19, 678–682, 1976.

Tomer, M. D., Dosskey, M. G., Burkart, M. R., James, D. E., Helmers, M. J., and Eisenhauer, D. E.: Methods to prioritize placement of riparian buffers for improved water quality, Agroforest. Syst., 75, 17–25, 2009.

White, M. J. and Arnold, J. G.: Development of a simplistic vegetative filter strip model for sediment and nutrient retention at the field scale, Hydrol. Process., 23, 1602–1616, https://doi.org/10.1002/hyp.7291, 2009.

Winchell, M. F., Jones, R. L., and Estes, T. L.: Comparison of models for estimating the removal of pesticides by vegetated filter strips, ACS Sym. Ser., ACS Publications, Washington, DC, 1075, 273–286, 2011.

Woolhiser, D. A., Smith, R. E., and Goodrich, D. C.: KINEROS, A kinematic runoff and erosion model: documentation and user manual, United States Department of Agriculture, Agricultural Research Service, ARS-77 March 1990, 130 pp., Washington DC, 1990.

Yang, J.: Convergence and uncertainty analyses in Monte-Carlo based sensitivity analysis, Environ. Modell. Softw., 26, 444–457, 2011.

Yu, C., Muñoz-Carpena, R., Gao, B., and Perez-Ovilla, O.: Effects of ionic strength, particle size, flow rate, and vegetation type on colloid transport through a dense vegetation saturated soil system: Experiments and modeling, J. Hydrol., 499, 316–323, https://doi.org/10.1016/j.jhydrol.2013.07.004, 2013.